

# FINITE ELEMENT INVESTIGATION OF THE SAFETY FACTOR OF TUNNEL PRIMARY LINING IN A DEEP TUNNEL UNDER SQUEEZING CONDITIONS

G. Antonucci & G. Scognamiglio

*Freelance, Lecce, Italy*

*Freelance, Naples, Italy*

**ABSTRACT:** This paper deals with a series of numerical simulations to investigate primary lining safety in deep tunnels under squeezing conditions. Finite element analyses are carried out by considering a circular shape tunnel under plain strain conditions, isotropic state of stress state, and elastoplastic Hoek & Brown criteria as constitutive law for the rock mass.

The numerical analysis carried out reproduces a complex geomechanical condition and evaluates the safety of a rigid temporary lining, consisting of HEB240 steel sets and shotcrete. The study aims to provide practical guidance to tunnel designers when excavation under squeezing rock mass conditions is expected.

## 1. INTRODUCTION

Squeezing rock conditions constitute a major challenge in mountain tunnelling, as documented by more than a century of experience (ANTONUCCI, G., BELLA, G., SCOGNAMIGLIO, G. 2024, SCOGNAMIGLIO, G. ANTONUCCI, G., BELLA, G. 2025). Squeezing is defined as a time-dependent large deformation of the rock mass surrounding the tunnel, primarily driven by creep processes activated when the shear stress exceeds a critical threshold. Deformations may either stabilize during construction or persist over long periods (BARLA, G. 1995). Tunnel convergence magnitude, deformation rate, and the extent of the yielded zone depend on geological conditions, the ratio between in situ stresses and rock mass strength, groundwater and pore pressure, and rock mass properties (STEINER, W. 1996). Squeezing behaviour is typically associated with weak, heavily jointed, and fractured rock masses, and is strongly influenced by overburden, with squeezing occurring once a critical depth is exceeded. Several deep tunnel case histories, such as the Saint Martin La Porte access adit and the Monte Ceneri Base Tunnel, illustrate these conditions. Squeezing response is closely linked to excavation methods and support installation sequences, making support selection a key factor for safety and design optimization. The aim of this study is to assess the safety factor of the temporary tunnel lining subjected to squeezing ground conditions, considering the influence of the installation distance from the tunnel excavation face.

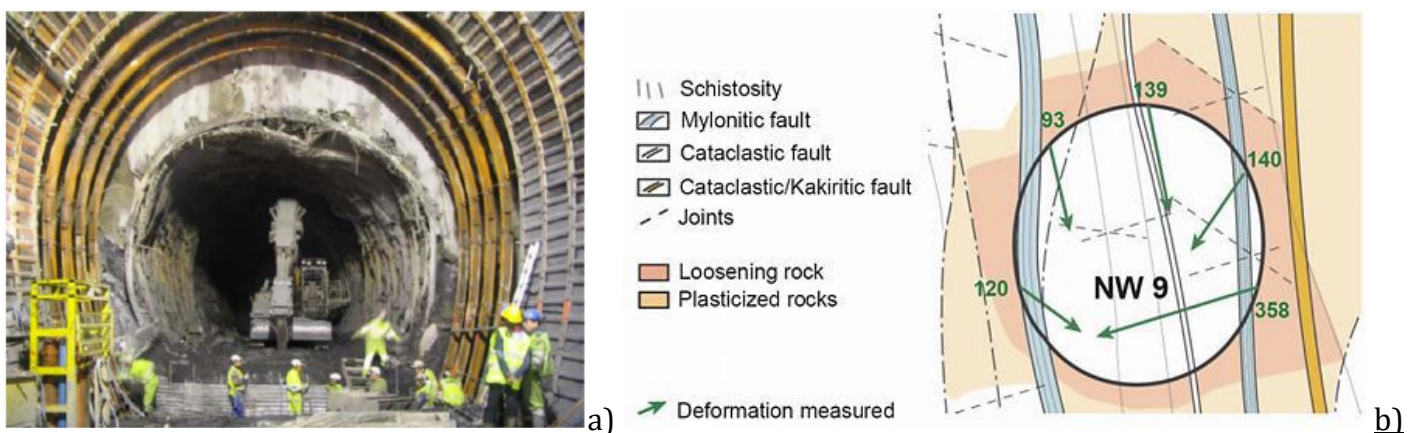


Figure 1: Relevant examples of squeezing occurrence: a) S. Martin la Porte ((BARLA, G. 1995)); b) Val Colla Line (MERLINI, D., STOCKER, D, FALANESCA M., SCHUERCH, R. 2018).

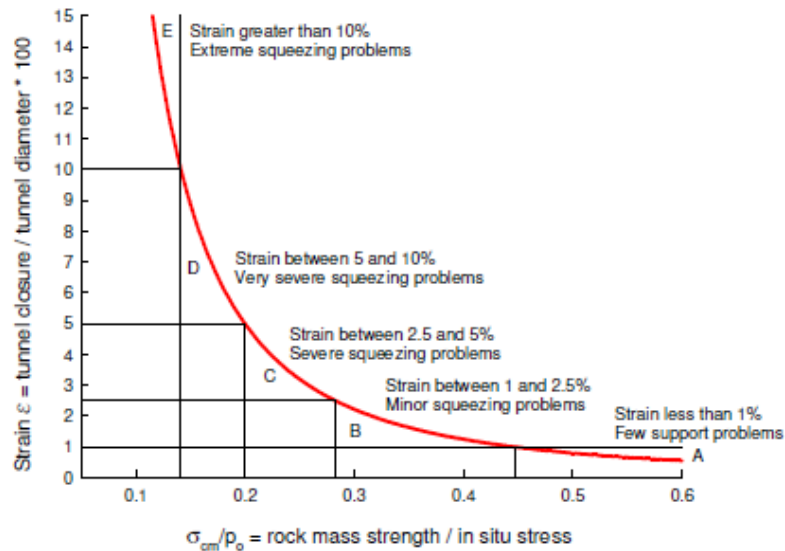


Figure 2: Classification of squeezing behaviour (HOEK E., MARINOS P. 2000)

## 2. NUMERICAL ANALYSIS

### 2.1 FINITE ELEMENT MODELLING AND HYPOTHESIS

A circular deep tunnel of radius  $R_T=5.0\text{m}$ , overburden  $H=600\text{m}$ , under a constant stress state and plane conditions was modelled by using the FE software RS2v.9.0 (RocScience). Triangular graded mesh, boundary conditions with hinges along all sides was adopted. Furthermore, the model sizes were set to avoid numerical side effects as shown in figure 3.

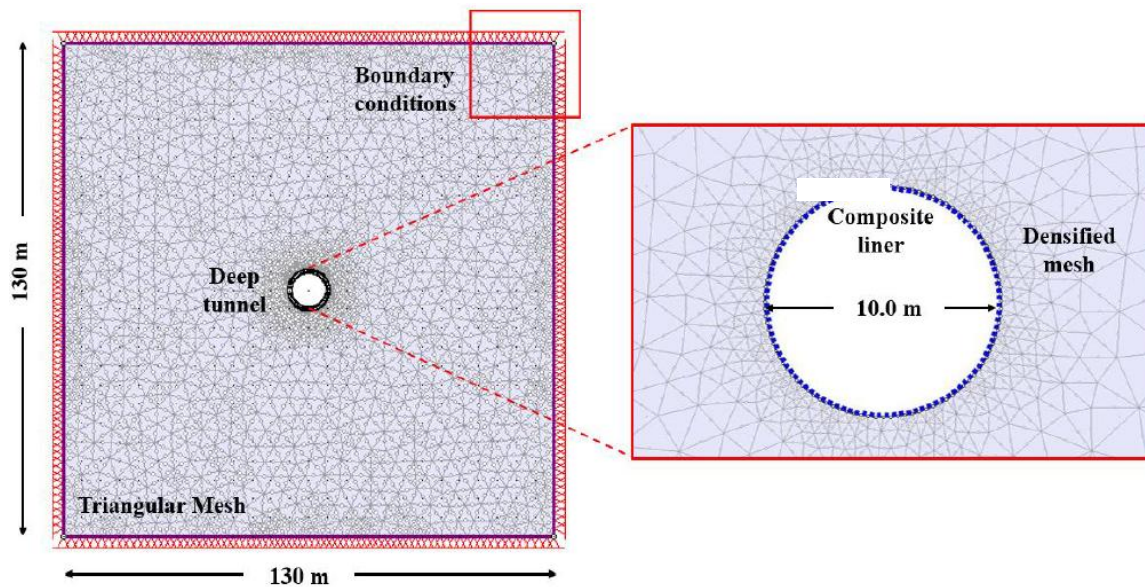


Figure 3: FE model, geometry, boundary conditions

The rock mass considered for analysis consist of Shists (average value  $MR=550$ ) and is characterized by an elastic perfectly plastic behaviour with generalized Hoek-Brown failure criteria. Knowledge of the uniaxial compressive strength (UCS) of the intact rock and the MR parameter makes it possible to estimate the elastic modulus of the intact rock (Eq. (1)) and, consequently, to derive the deformability modulus of the rock mass as a function of the GSI and the disturbance factor D (Eq. (2)). Furthermore, the assessment of squeezing behaviour requires the determination of the rock mass uniaxial compressive strength ( $\sigma_{cm}$ ) according to Eq. (3) proposed by (HOEK E., MARINOS P. 2000), which depends on the Hoek-Brown parameter, the uniaxial compressive strength of the intact rock, and the Geological Strength Index.

$$E_i = MR \cdot UCS \quad (1)$$

$$E_d = E_i \left( 0.02 + \frac{1 - D/2}{1 + e^{((60+15D-GSI)/11)}} \right) \quad (2)$$

$$\sigma_{cm} = (0.0034 m_i^{0.8}) \sigma_{ci} [1.029 + 0.025 e^{(-0.1m_i)}]^{GSI} \quad (3)$$

Isotropic state of stress and dry conditions were assumed, the geomechanics parameters indicated in Table 1 are typical of extreme squeezing phenomena ( $\sigma_{cm}/p_0 < 0.10$ ) according to Figure 2.

Table 1: Rock-mass parameters. ( $\gamma=27$  kN/m<sup>3</sup>,  $\nu=0.30$   $p_0=16.2$ MPa,  $k_0=1$ ,  $D=0$ )

Rock-mass parameters							
	MR [-]	UCS [MPa]	GSI [-]	$m_i$ [-]	$E_d$ [MPa]	$\sigma_{cm}$ [MPa]	$\sigma_{cm}/p_0$ [-]
Analysis A-B	550	12	30	20	537	1.17	0.07

The tunnel excavation was simulated step-by-step by calculating the relaxation factor  $\lambda(X)$  according to the convergence-confinement method. The computation stages used to performing the numerical analysis are shown in the following table.

Table 2: Finite element stages with indication of ratio  $p_i/p_0=(1-\lambda)$  and distance from tunnel face (X)

Stage n.	Description
1	In situ state of stress, $p_i/p_0=1,0$
2	Tunnel face excavation, $X=0m - p_i(X)/p_0$
3	Temporary lining installation, $X=(0.5-3.0m) - p_i(X)/p_0$
4	Tunnel excavation advance, $X=5,0m - p_i(X)/p_0$
5	Section far from tunnel face, $p_i/p_0=0,0$

The aim of the numerical analyses carried out (Analysis A and B) is to evaluate the safety factor of the primary lining as a function of the distance from the tunnel excavation face at which it is applied (X). Specifically, both analyses consist of six cases each (Case 1: X = 0.5 m, Case 2: X = 1.0 m, Case 3: X = 1.5 m, Case 4: X = 2.0 m, Case 5: X = 2.5 m, Case 6: X = 3.0 m). In the numerical analysis, the primary lining was modelled as a element type "reinforced concrete" that includes as 0.20m thick shotcrete layer and HEB240 steel ribs spaced at 1.0m interval.

Table 3: Primary-lining parameters. Steel ribs: type and spacing (s); shotcrete: thickness ( $h_{sh}$ ), elastic modulus ( $E_{sh}$ ), Poisson's ratio ( $\nu$ ), compressive strength ( $\sigma_{sh}$ )

	Primary lining					
	Steel ribs		Shotcrete			
	Type [-]	s [m]	$h_{sh}$ [m]	$E_{sh}$ [MPa]	$\nu$ [-]	$\sigma_{sh}$ [MPa]
Analysis A	HEB240	1.00	0.20	5000	0.15	30
Analysis B	HEB240	1.00	0.20	25000	0.15	30

As can be seen from Table 1, the difference between Analysis A and Analysis B concerns the elastic modulus of the shotcrete: Analysis A simulates fresh concrete, while Analysis B simulates a concrete with mechanical properties corresponding to a curing age of 7 days.

## 2.2 DESIGN APPROACH

Finite element analyses are performed to evaluate the safety level of the primary lining as a function of the distance from the tunnel face, as follows:

1. A 2D convergence–confinement analysis was performed on the unsupported tunnel using n. 10 calculation phases ( $p_i/p_0=1.0, 0.8, 0.4, 0.2, 0.1, 0.08, 0.04, 0.02, 0.01$  and 0). From the final stage, the maximum convergence ( $u_{max}$ ) and the plastic radius ( $R_p$ ) were determined (Fig.4b top);
2. The method proposed by (VLACHOPOULOS N., M.S. DIEDERICHS, M.S. 2009) allows the determination of tunnel convergence ( $u_r$ ) at the relevant distances from the tunnel face (X) through the knowledge of  $R_p/R_T$  ratio, as shown in figure 4a;
3. according to the convergence-confinement method (PANET M., GUENOT, A. 1982 ), radial displacements allow the evaluation of the ratio  $p_i/p_0=(1-\lambda)$  at the tunnel face and at the section where the temporary lining is installed, as provided in Fig.4b-bottom;
4. The knowledge of the relaxation factors  $\lambda(X)$  made it possible to perform finite element (FE) numerical analyses and compare the results obtained for the two models performed (analysis A and B). Each analyses was computed from  $X=0.5m$  to  $3.0m$  (case n. 1  $\rightarrow$  case n. 6) through n. 5 calculation stages.

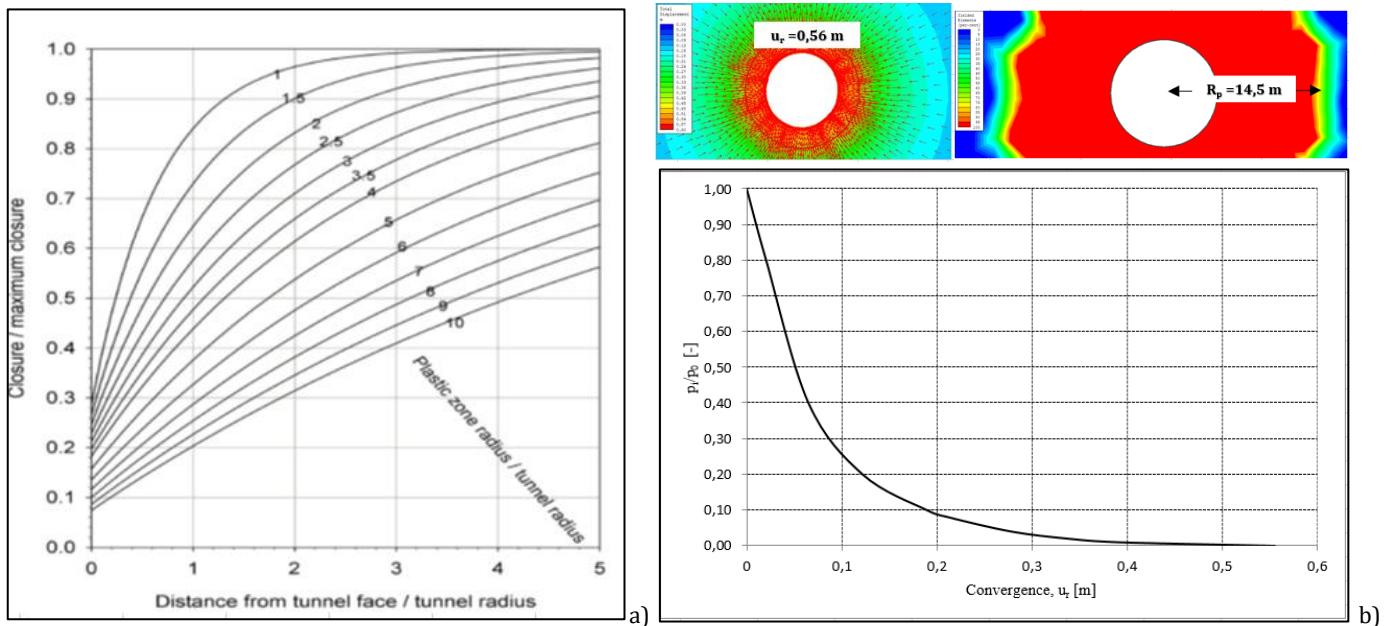


Figure 4: a) solution proposed by (VLACHOPOULOS N., M.S. DIEDERICHS, M.S. 2009) to estimate the tunnel convergence and different tunnel face distances; b) top: maximum convergence and plastic radius of the unsupported tunnel by analysis 2D; b) bottom: evaluation of the ratio  $p_i/p_0$ , and so the relaxing factor from the ground reaction curve

### 3. RESULTS

The main outcomes are presented in the following section. A comparison between the numerical results obtained from FE analyses considering temporary lining Type A and Type B is reported in Tables 4 and 5. The comparison is carried out in terms of maximum convergence at the time of lining installation ( $u_x$ ), plastic radius ( $R_p$ ), characteristic values of the maximum axial force ( $N_{max}$ ) and maximum bending moment ( $M_{max}$ ), as well as the safety factor at lining installation (SF).

Table 4: Results numerical analysis A: maximum convergence at temporary lining installation ( $u_x$ ), plastic radius ( $R_p$ ), maximum axial force ( $N_{max}$ ), maximum bending moment ( $M_{max}$ ) and safety factor (SF) .

Analysis A	Primary lining: HEB240/1m - $E_{sh}=5000\text{MPa}$					
	X [m]	$u_x$ [mm]	$R_p$ [m]	$N_{max}$ [MN]	$M_{max}$ [MNm]	SF (-)
Case 1	0.5	0,225	7,1	3	0,007	2,00
Case 2	1.0	0,227	7,2	4,7	0,007	1,25
Case 3	1.5	0,232	7,4	7,5	0,007	0,80
Case 4	2.0	0,235	7,5	9,3	0,007	0,62
Case 5	2.5	0,237	7,7	10,4	0,008	0,57
Case 6	3.0	0,237	7,7	10,7	0,009	0,57

Table 5: Results numerical analysis B: maximum convergence at temporary lining installation ( $u_x$ ), plastic radius ( $R_p$ ), maximum axial force ( $N_{max}$ ), maximum bending moment ( $M_{max}$ ) and safety factor (SF).

Analysis B	Primary lining: HEB240/1m $E_{cls}=25000\text{MPa}$					
	X [m]	$u_x$ [mm]	$R_p$ [m]	$N_{max}$ [MN]	$M_{max}$ [MNm]	SF (-)
Case 1	0.5	0,222	7	3,2	0,004	4,00
Case 2	1.0	0,224	7,15	5,1	0,005	2,67
Case 3	1.5	0,226	7,2	8,1	0,005	1,60
Case 4	2.0	0,228	7,2	9,9	0,006	1,33
Case 5	2.5	0,227	7,2	11,1	0,006	1,25
Case 6	3.0	0,228	7,2	11,5	0,008	1,14

For conservative purposes, the resistance domain was evaluated by considering exclusively the contribution of the HEB240 steel sets with a spacing of 1 m, neglecting the contribution of shotcrete. The interaction diagrams show that, in Analysis A, only cases 1 and 2 ( $X = 0.5$  m and  $X = 1.0$  m) satisfy the resistance criteria, whereas in Analysis B, characterised by the use of shotcrete with enhanced mechanical properties, all analysed cases (1–6) fall within the resistance domain. This behaviour can be attributed to the increase in the overall stiffness of the support system induced by the shotcrete ( $E_{sh} = 25,000$  MPa compared to 5,000 MPa), which results in a significant reduction of the stresses acting on the steel sets. The parametric analyses further highlight a decrease in the safety factor with increasing distance from the excavation face; however, for a given steel set geometry and distance from the face, the contribution of shotcrete proves to be decisive in ensuring safety factors greater than unity. Finally, for the geomechanical conditions analysed, the plot reported in Figure 7 indicates that, in order to increase the excavation advance without compromising the structural safety of the lining, the adoption of a double round length of 1.0 m ( $X = 2.0$  m) can be envisaged, provided that a temporary lining with adequate mechanical properties is employed.

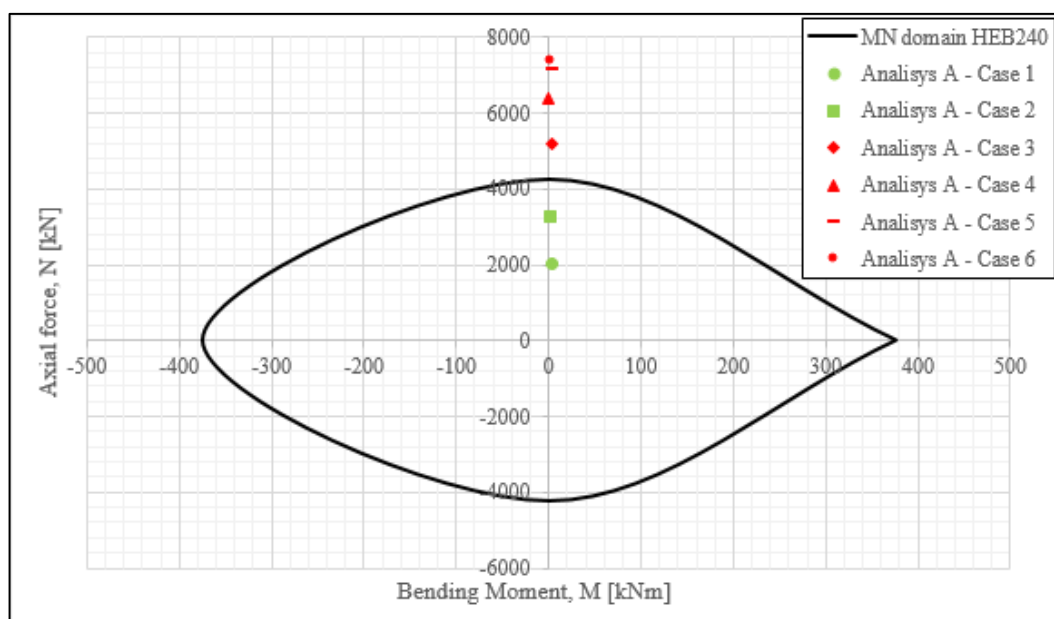


Figure 5: Interaction MN diagram in the case Analysis A

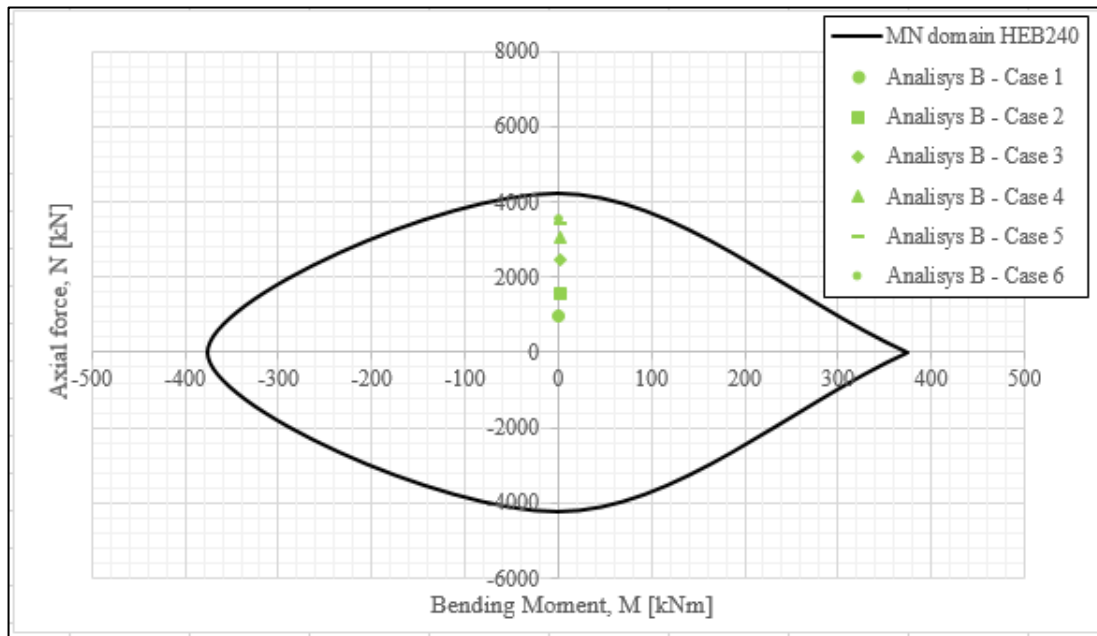


Figure 6: Interaction MN diagram in the case Analysis B

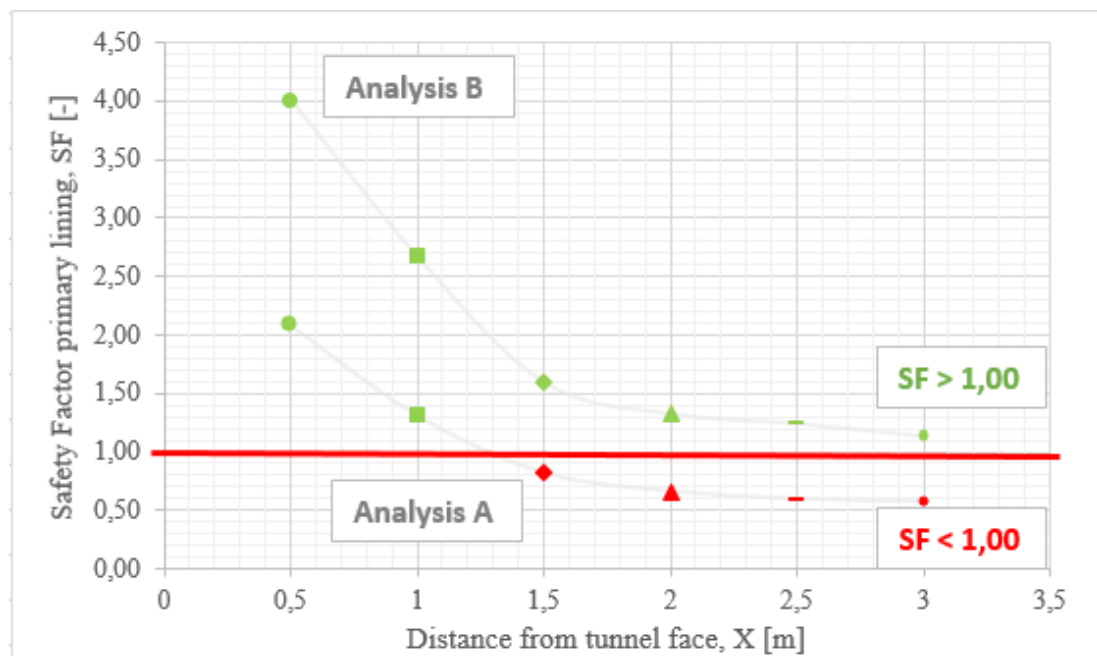


Figure 7: Primary lining safety factor versus distance from the tunnel face, X, for Analyses A (lower curve) and B (upper curve).

#### 4. CONCLUSION

The analyses carried out indicate that delays in the installation of the primary support system, as a function of the distance from the excavation face, have a significant influence on the tunnel stress–strain response. In particular, delayed installation of steel sets, coupled with shotcrete with insufficient mechanical performance, leads to increased cavity deformations—expressed in terms of convergence—and to the mobilisation of higher induced stress levels. Within this context, the implementation of a properly designed internal monitoring system is essential. The integrated use of face extrusometers, pressure cells, and extensometers mounted on the steel sets, together with topographic targets for convergence measurements, allows continuous monitoring of the stress–strain evolution and the evaluation of the effectiveness of the primary lining, thus providing a robust validation of the design assumptions and predictions.

## LITERATURE

- ANTONUCCI, G., BELLA, G., SCOGNAMIGLIO, G. *Numerical Analysis of Tunnel Supports in Weak Ground Conditions and High Stress Levels*, Proceeding of the 5th International Conference on Civil Engineering Fundamentals and Applications (ICCEFA024), Lisbon, Portugal, vol. 01, pp. 1-8, 2024.
- SCOGNAMIGLIO, G. ANTONUCCI, G., BELLA, G.. *On the stress-strain response of deep tunnel in squeezing conditions: numerical analysis for the design of rock supports*, Proceeding of the 10th International Conference on Geotechnical Research and Engineering (ICGRE 2025), Barcelona, Spain, vol. 01, pp. 1-8, 2025.
- BARLA, G. *Squeezing rocks in tunnels*. ISRM News Journal, 3/4, pp. 44-49, 1995.
- STEINER, W. *Tunnelling in squeezing rocks: case histories*. Rock Mech. and Rock Eng., vol. 29, pp. 211-246, 1996.
- BARLA, G. *Innovative tunneling construction method to cope with squeezing at the Saint Martin La Porte access adit (Lyon-Turin Base Tunnel)*. Proceedings of the Eurock 2009 Rock Engineering in Difficult Ground Conditions, Dubrovnik, Croatia, 2009, vol. 1, pp. 1-10.
- MERLINI, D., STOCKER, D, FALANESCA M., SCHUERCH, R. *The Ceneri Base Tunnel: Construction experience with the Southern Portion of the Flat Railway Line Crossing the Swiss Alps*, Engineering, vol. 1, no. 02, pp. 235-248, 2018.
- HOEK E., MARINOS P. *Predicting tunnel squeezing problems in weak heterogeneous rock masses*, Tunnels and Tunnelling International, vol. 32, no. 11, pp. 45-51, 2000.
- KOVÁRI, K., AMSTAD,C., ANAGNOSTOU, G. *Design / Construction methods Tunnelling in swelling rocks*, Proceeding of the 29th U.S. Symposium Key Questions in Rock Mechanics, Minnesota, pp. 17-32, 1988.
- SCHUBERT, W. *Dealing with Squeezing Conditions in Alpine Tunnels*, Rock Mech Rock Eng, vol. 29, no. 03, pp.145-53, 1996.
- KOVÁRI, K. *Method and device for stabilizing a cavity excavated in underground construction*. US Patent 20050191138, 2005.
- VLACHOPOULOS N., M.S. DIEDERICHS, M.S. *Improved longitudinal displacement profiles for convergence confinement analysis of deep tunnels*, Rock Mechanics and Rock Engineering, vol. 42, no. 02, pp. 131-146, 2009.
- PANET M., GUENOT, A. *Analysis of convergence behind the face of a tunnel*, Proceeding of the International Symposium Tunnelling, (IST'82), The Institution of Mining and Metallurgy, London, pp. 197-204, 1982.
- BELLA, G., ANTONUCCI G., SCOGNAMIGLIO, G. *Finite Element Investigation on the Response of Tunnel Rock-Supports in Zones Subjected To Squeezing Occurrence*, Avestia Publishing International Journal of Civil Infrastructure (IJCI) Volume 8, Year 2025.

**Eng, Giulio Antonucci: Author1**

**Affiliation: Freelance**

**E-mail address: [ing.antonuccigiulio@libero.it](mailto:ing.antonuccigiulio@libero.it)**

**Eng, Gennaro Scognamiglio: Author2**

**Affiliation: Freelance**

**E-mail address: [ing\\_scognamiglio@libero.it](mailto:ing_scognamiglio@libero.it)**